Research Article

A Two-Step SO₃H/ICG Catalyst Synthesis for Biodiesel Production: Optimization of Sulfonation Step *via* Microwave Irradiation

Nur Nazlina Saimon, Norzita Ngadi, Mazura Jusoh, Zaki Yamani Zakaria*⁾

School of Chemical & Energy Engineering, Faculty of Engineering, Universiti Teknologi Malaysia, Skudai 81310, Malaysia.

Abstract

Conventional heating, a common method used for heterogeneous solid acid catalyst synthesis unknowingly consumes massive time and energy. In this study, acid catalyst was prepared through sulfonation process of incomplete carbonized glucose (ICG) via microwave-assisted technique to shorten the heating time and energy consumption. Optimization of the sulfonation process of ICG via microwave-assisted was carried out. Four-factor-three-level central composite design (CCD) was used to develop the design of experiments (DOE). Interaction between two factors was evaluated to determine the optimum process conditions. A quadratic model was proposed for prediction of biodiesel yield (Y) from palm fatty acid distillate (PFAD) and its conversion (C). The application of DOE successfully optimized the operating conditions for the two-step SO₃H/ICG catalyst synthesis to be used for the esterification process. The optimized conditions of the best performing SO₃H/ICG with maximum Y and C were at 7.5 minutes of reaction time, 159.5 mL of H₂SO₄ used, 671 rpm of stirring rate as well as 413.64 watt of power level. At these optimum conditions the predicted yield percentage and conversion percentage were 94.01% and 91.89%, respectively, which experimentally verified the accuracy of the model. The utilization of sulfonated glucose solid acid catalyst via microwave-assisted in biodiesel production has great potential towards sustainable and green method of synthesizing catalyst for biodiesel.

1. Introduction

The process optimization in biodiesel production depends on independent variable process parameters, such as: percentage weight of the catalyst (wt%), molar ratio of alcohol to oil, reaction temperature (°C) as well as reaction time (min) [1]. However, there is lack of study in optimizing the independent variable during the preparation of the heterogeneous acid catalyst for biodiesel production itself. This catalyst preparation segment is imperative in biodiesel production in order to further reduce time and energy consumption for its synthesis since it possess high recyclability and are applied extensively in a conventional way. Zong [2] and Lokman [3] did great work in functionalizing the

* Corresponding Author.
  Email: zakiyamani@utm.my (Z.Y. Zakaria);
  Telp: +607-535553

carbonized D-glucose using sulfuric acid in the esterification of high FFA feedstock for biodiesel production. However, both study reported that the time to sulfonate or functionalize the carbonized d-glucose required almost 15 h which consumed a lot of time and energy as well. Previous study by Shuit and Tan [4] modified the sulfonation method for multi walled carbon nano-tubes (MWCNTs) thermal decomposition and thermal treatment under nitrogen gas (N_2) flow for esterification of palm fatty acid distillate (PFAD). Optimization of these parameters was often done traditionally by using one-factor-at-a-time (OFAT) method where one factor is varied while the other factors are kept constant. This method is tedious if it involves large number of parameters.

Optimization using design of experiments (DOE) is more efficient statistically when dealing with more than 3 variables. Many researchers used DOE for optimizing their biodiesel production from high free fatty acid (FFA) feedstock such as waste frying oil [5], animal fats [6] as well as PFAD [7]. Most of the investigations optimized the variables of the biodiesel production for esterification including catalyst loading (wt%), reaction temperature (°C), molar ratio of alcohol to oil, as well as reaction time (min). Although the optimizations for esterification for biodiesel production were well covered by researchers, the optimization for heterogeneous solid catalyst synthesis is not sufficiently dealt with. If the solid catalyst is well optimized for the sulfonation stage, massive benefit could be attained and this can lead biodiesel production to be more commercially viable. Besides systematically optimizing the synthesis of SO_3H/ICG catalyst, microwave irradiation was utilized to enhance the rate of heating which will rapidly speed up the duration of catalyst preparation. To the best of our knowledge, the application of microwave irradiation for biodiesel catalyst synthesis context via DOE has not been reported by others. Therefore, the main purpose of this study is to optimize the sulfonation variables including the volume of H_2SO_4 (mL), sulfonation time (min), power level of microwave (W) and power stirring (rpm). Central Composite Design (CCD) of RSM in Design Expert 7th version was employed for optimization for the sulfonation of the incomplete carbonized glucose (ICG). CCD was chosen because it is commonly applied in designing sequential experimental which consists of multivariate equations. The multivariate equations is simultaneously resolved by manipulations of the quantitative data in experimental design of the RSM [8]. This method

has practically applied to determine the optimum conditions since RSM offers efficient and easier method compared to the conventional OFAT experiment design.

2. Materials and Methods

2.1 Materials

Main chemical used was D-(+) Glucose (100% purity) which had been bought from QRec (Asia) Sdn. Bhd. The PFAD used for catalytic performance was supplied by Mewaholeo Industries Sdn. Bhd., Pasir Gudang, Malaysia. Methanol (99.9% purity) and H_2SO_4 (98.0% purity) was supplied from Merck and J.T. Baker, US, respectively. Gas chromatography (GC) Flame Ionization Detector (FID) Agilent brand and N7890 model was employed for the quantification. Methyl ester's standard for GC analysis, such as: methyl linoleate, methyl myristate, methyl oleate, methyl palmitate, and methyl stearate, were purchased from Sigma-Aldrich chemical company. All analytical grade products for all chemicals required no further purification. Equipment employed for catalyst preparation is Microwave SHARP R213CST.

2.2 Catalyst Preparation

20 g of D(+)-Glucose powder was melted through heating process in a microwave for 20 minutes at medium power level (400 W). The ICG formed was then crushed into powder form and sieved at 150 nm. 4 g of the crushed ICG was added with 100 mL of concentrated H2SO4 and stirred at 500 rpm for 5 minutes for sulfonate introduction to the glucose based. The mixture was then heated inside a microwave in medium high power level for sulfonation process for certain respective reaction times. The mixtures was then filtered and black precipitate was collected before washing process using hot distilled water at 85 °C to remove impurities contained in the mixture. Finally the catalyst was dried inside an oven for 5 hours to remove the moisture content in the catalyst.

2.3 Methyl Ester Production

FFA of PFAD can be reduced through esterification process. PFAD were weighed based on molar ratio and properly heated at 65 °C. Preheated PFAD was poured into a three neck round bottom flask following by the methanol and catalyst. Molar ratio of PFAD and methanol used was 10:1. 2.5 wt% of sulfonated glucose loading was used for the esterification.

The mixture was then refluxed to 70 °C for 90 minutes and poured into a separating funnel to settle for 3 hours. The biodiesel layer was then separated from the catalyst and the mass of the biodiesel produced from the esterification was weighed to calculate the biodiesel percentage yield.

2.4 Analysis of PFAD Methyl Ester

The percentage yield of biodiesel was calculated using Equation 1. Biodiesel in this study is defined as the top 5 components which are methyl linoleate, methyl myristate, methyl oleate, methyl palmitate and methyl stearate. From the esterification reaction, only methyl esters were obtained and no other compounds were present. The conversion of the biodiesel was determined through acid-base titration method. About 1 mL of biodiesel was added into 20 mL of the solvent, methanol. The mixture was then shaken until it dissolved. 2–3 drops of phenolphthalein was added into the flask and titrated with standardized potassium hydroxide (KOH) solution until the first permanent pink color showed up. The formula to calculate the percentage yield, acid value and percentage conversion were defined by equation (1), (2) and (3), respectively.

$$Yield(\%) = \frac{weight\ of\ experimental\ biodiesel\ (g)}{weight\ of\ theoretical\ biodiesel\ (g)} \times 100 \quad (1)$$

$$Acid\ value = \frac{N \times MW\ KOH \times Volume\ of\ KOH\ titrate\ used\ (mL)}{mass\ of\ biodiesel\ (g)} \quad (2)$$

where, N refers to the normality of KOH used and MW indicating the molecular weight of KOH which is 56.11 g/mol.

$$Conversion(\%) = \frac{(acid\ value\ of\ PFAD - acid\ value\ of\ sample)}{acid\ value\ of\ PFAD} \times 100 \quad (3)$$

2.5 Optimizing Using CCD (Central Composite Design)

In this study, four factors Central Composite Design (CCD) require 30 experiments to be run, which includes six center points, six axial points, and eight factorial points. Yield and conversion response were analyzed to evaluate the performance of the process conducted. To produce experimental design for the synthesis of SO_3H/ICG catalyst, heating time of catalyst, volume of H_2SO_4 used, power level and stirring rate were chosen as parameters that influence the efficiency of catalyst produced.

The fitness and adequacy of the models were validated using F-values, P values and affirmed further by the R^2 value. Models achieving 95% confidence interval indicates acceptable accuracy. Some parts of the analysis were discussed and related to catalyst characterization results. The catalyst characterization are not discussed here but is referred to our previous report [10].

3. Results and Discussion

3.1 Single Response Optimization for Yield (Y) and Conversion (C)

In this chapter, five level of four factorial CCD were selected because it can fit a full quadratic model. CCD provides a factorial design with center points, augmented with a group of axial points which can estimate curvature. This level requires 30 series of experimental design including six center points, 6 axial points as well as 8 factorial points. The responses of this optimization were percentage yield of FAME and percentage of conversion of FFA in PFAD. Four independent variables used in sulfonation of the ICG were sulfonation time (X_1), volume H_2SO_4 (X_2), power level of microwave (X_3), as well as stirring rate (X_4). These 4 parameters were selected based on the most significantly variables influencing the catalytic activity as well as from previous study [9]. Table 1 tabulates experimental level coded and range for independent variables. The level coded ranging from the lowest ($-\alpha$) to the median to the highest ($+\alpha$). Time labelled as X_1 was ranging from 3 to 11 min, volume of H_2SO_4 (X_2) was from 50 mL to 250 mL, power level of microwave (X_3) from 80 W to 720 W and stirring rate (X_4) from 200 rpm to 1000 rpm. Saimon and colleagues managed to obtain high percentage yield of FAME 91.41% using 100 mL of H_2SO_4 at 7 min of sulfonation time and 560 W of microwave's power level [10]. Thus,

Table 1. Experimental level coded and range of independent parameters.

Parameter	$-\alpha$	-1	0	$+1$	$+\alpha$
Time, X_1 (min)	3	5	7	9	11
Volume H_2SO_4, X_2 (mL)	50	100	150	200	250
Power Level, X_3 (watt)	80	240	400	560	720
Stirring rate, X_4 (rpm)	200	400	600	800	1000

the ranges were extended to determine the optimum value for these independent variables. The respective catalyst characterizations for this investigation that include XRD, BET, SEM, FTIR and TPD−NH₃ have been reported earlier [10].

As mentioned earlier, the responses of yield (*Y*) as well as conversion (*C*) were investigated using multiple regression analysis. Second order polynomial [11] was applied in this analysis as presented by Equation (4) as follow:

$$y = \beta_o + \sum_{i=1}^{3}\beta_i x_i + \sum_{i=1}^{3}\beta_i x_i^2 + \sum_{i=1}^{2}\sum_{j=i+1}^{3}\beta_{ij}x_i x_j \quad (4)$$

where *y* is the percentage yield of FAME or percentage of FFA conversion; x_i and x_j are the independent variables and β_o, β_i, β_{ii}, β_{ij} are intercept, linear, quadratic as well as interaction constant coefficients respectively.

The DOE complete with the independent variables as well as responses experimental and predicted are tabulated in Table 2. The interaction of the independent variables and the responses are derived as shown in Equation (5) and Equation (6).

$$\begin{aligned} Y = {} & 93.20 + 1.346X_1 + 1.53X_2 + 0.55X_3 + 1.48X_4 \\ & + 0.18X_1X_2 + 0.68X_1X_3 - 0.076 + 0.089X_2X_3 \\ & + 0.081X_2X_4 - 0.4X_3X_4 - 1.91X_1^2 - 2.83X_2^2 \\ & - 3.52X_3^2 - 1.21X_4^2 \end{aligned} \quad (5)$$

$$\begin{aligned} C = {} & 91.40 + 1.36X_1 + 1.31X_2 + 0.64X_3 + 1.45X_4 \\ & + 0.10X_1X_2 + 0.70X_1X_3 + 0.20X_1X_4 \\ & - 0.19X_2X_3 - 0.096X_3X_4 - 3.17X_1^2 \\ & - 4.02X_2^2 - 4.50X_3^2 - 2.54X_4^2 \end{aligned} \quad (6)$$

Table 2. Design of experiments of sulfonation of ICG for esterification of PFAD.

Run	X_1	X_2	X_3	X_4	Yexp (%)	Y RSM (%)	Cexp (%)	C RSM (%)
1	5	100	240	400	80.72	79.55	74.21	72.91
2	7	150	400	200	84.47	85.39	77.65	78.35
3	7	50	400	600	78.21	78.82	71.90	72.70
4	5	100	560	800	81.08	82.05	74.54	75.67
5	9	100	560	800	85.33	85.59	81.20	80.41
6	5	100	560	400	79.52	79.9	73.10	73.36
7	7	150	80	600	77.41	78.68	71.16	72.11
8 c	7	150	400	600	92.43	93.20	90.51	91.40
9	11	150	400	600	87.34	88.24	80.29	81.44
10	5	200	560	800	84.62	85.10	77.79	78.13
11	7	150	400	1000	92.17	91.29	84.73	84.16
12 c	7	150	400	600	93.51	93.20	91.76	91.40
13 c	7	150	400	600	92.85	93.20	90.31	91.40
14	5	200	240	400	81.45	81.92	74.88	76.13
15	9	200	560	400	86.54	87.18	79.01	79.34
16 c	7	150	400	600	93.54	93.20	92.43	91.40
17	9	100	560	400	84.72	83.74	77.88	77.3
18	9	200	240	400	85.46	83.74	78.56	76.84
19	9	200	240	800	87.16	87.50	80.13	80.34
20 c	7	150	400	600	94.01	93.20	92.76	91.40
21	3	150	400	600	83.75	82.89	76.99	75.98
22	9	100	240	800	85.11	84.09	78.24	77.54
23	9	100	240	400	80.41	80.65	73.92	74.04
24	5	200	560	400	82.36	82.63	75.71	75.82
25	5	200	240	800	85.76	85.98	78.84	78.83
26	7	250	400	600	85.52	84.95	78.62	77.96
27	5	100	240	800	83.21	83.29	75.48	75.61
28	7	150	720	600	82.11	80.88	75.48	74.67
29 c	7	150	400	600	92.84	93.20	90.63	91.40
30	9	200	560	800	88.93	89.35	81.75	82.45

c: Centre value of all parameters.

Table 3. Analysis of variance (ANOVA) for yield response of biodiesel production.

Source	Sum of Squares	df	Mean Square	F Value	p-value Prob > F	Comments
Model	672.62	14	48.04	41.16	< 0.0001	significant
X_1	42.99	1	42.99	36.83	< 0.0001	
X_2	56.43	1	56.43	48.34	< 0.0001	
X_3	7.28	1	7.28	6.24	0.0246	
X_4	52.27	1	52.27	44.78	< 0.0001	
X_1X_2	0.51	1	0.51	0.44	0.5181	
X_1X_3	7.48	1	7.48	6.41	0.0230	
X_1X_4	0.093	1	0.093	0.080	0.7816	
X_2X_3	0.13	1	0.13	0.11	0.7470	
X_2X_4	0.11	1	0.11	0.090	0.7677	
X_3X_4	2.54	1	2.54	2.18	0.1605	
X_1^2	99.91	1	99.91	85.59	< 0.0001	
X_2^2	219.45	1	219.45	188.00	< 0.0001	
X_3^2	308.70	1	308.70	264.46	< 0.0001	
X_4^2	40.48	1	40.48	34.68	< 0.0001	
Residual	17.51	15	1.17			
Lack of Fit	15.80	10	1.58	4.61	0.0527	Not significant
Pure Error	1.71	5	0.34			
Cor Total	690.13	29				
R-square = 0.9746 ; Adjusted R-square = 0.9510						

Table 4. Analysis of variance (ANOVA) for conversion response of biodiesel production.

Source	Sum of Squares	df	Mean Square	F Value	p-value Prob > F	Comments
Model	1201.66	14	85.83	60.76	< 0.0001	significant
X_1	44.66	1	44.66	31.62	< 0.0001	
X_2	41.45	1	41.45	29.34	< 0.0001	
X_3	9.83	1	9.83	6.96	0.0186	
X_4	50.63	1	50.63	35.84	< 0.0001	
X_1X_2	0.18	1	0.18	0.12	0.7287	
X_1X_3	7.92	1	7.92	5.61	0.0317	
X_1X_4	0.64	1	0.64	0.45	0.5111	
X_2X_3	0.57	1	0.57	0.40	0.5349	
X_2X_4	0.000	1	0.000	0.000	1.0000	
X_3X_4	0.15	1	0.15	0.10	0.7505	
X_1^2	276.21	1	276.21	195.52	< 0.0001	
X_2^2	442.89	1	442.89	313.52	< 0.0001	
X_3^2	556.25	1	556.25	393.76	< 0.0001	
X_4^2	176.38	1	176.38	124.86	< 0.0001	
Residual	21.19	15	1.41			
Lack of Fit	15.58	10	1.56	1.39	0.3772	Not significant
Pure Error	5.61	5	1.12			
Cor Total	1222.58	29				
R-square = 0.9872 ; Adjusted R-square = 0.9665						

Based on the Equations (5) and (6), the effect of particular factor is respectively shown by the individual factor (X_1, X_2, X_3 and X_4) meanwhile the interaction between two factors is presented by the quadratic effects of the two factors (X_1X_2, X_1X_3, X_1X_4, X_2X_3, X_2X_4, X_3X_4, X_1^2, X_2^2, X_3^2, and X_4^2). The positives and negatives sign for each codes represent the parallel effects and adverse effects towards the responses respectively. Highest orders of polynomials was selected for this model indicates that the models are significant.

Regression model equation generated from the RSM is capable to analyze the adequacy of the model. The adequacy of the model indicates the interactions between the variables to the responses. The determination coefficient which also known as R^2 value is the most important factor to determine the appropriateness of the model adequacy through the revelation of the total variation of the mean observed of the system [12]. Table 3 and Table 4 show the sequential model sum of squares for the experimental design for both yield and conversion responses. The tables tabulate F-value, the significance of the model, the lack of fit as well as the R^2 value for responses yield as well as conversion.

The R^2 value for Y and C were 0.9746 and 0.9827, respectively indicated that high precision as well as the adequacy of the model developed. High value of R^2 describes a good validity of the models generated. Both of the R^2 values indicate 97.46% and 98.27% from the sample were attributed to the variables meanwhile the remaining 2.54% and 1.73% of Y and C respectively could not be explained by the regression model. The close agreement between the R^2 value and adjusted R^2 value for both Y and C describes the related variables of the model. The

percentage of coefficient of variation (C.V.) were 1.26% and 1.49% for both Y and C response indicates a high reliability between fitted model and the experimental results [13].

Evaluation of the variance or the regression model's adequacy can be obtained by using ANOVA. ANOVA is a statistical method to determine the differences between two or more means and evaluating the important effect between all variables and responses in order to fit with the second order polynomials model developed along with the experimental value. F value is the most important value to be observed. F-value indicates the ratio of mean square based on the regression to the mean square to residual error. Significant F-value is obtained when the value is higher than the model's tabulated value. From Table 3 and 4, F-value for both Y and C were 41.16 and 60.76, respectively. 5.27% and 37.72% of chance of error were reported for both Y and C, respectively. The low value of the chance of error indicating that it is non-significant toward the model where it is a good sign since the model is required to be fit with a second order polynomial model.

The variables or parameters used for Y and C responses can be significantly observed via ANOVA. For Y response, parameter of volume of H_2SO_4 is found to be the most significant or provide high influence on yield production. The F-value for this parameter is 48.34 with p-value less than 0.001. For C on the other hand, it is found that stirring rate gives the highest F-value with 35.84 with p-value less than 0.001 to significantly affect the conversion percentage in biodiesel production. Due to the polar and nonpolar nature of sulfuric acid and D(+)-Glucose, the sulfonation suffers initial
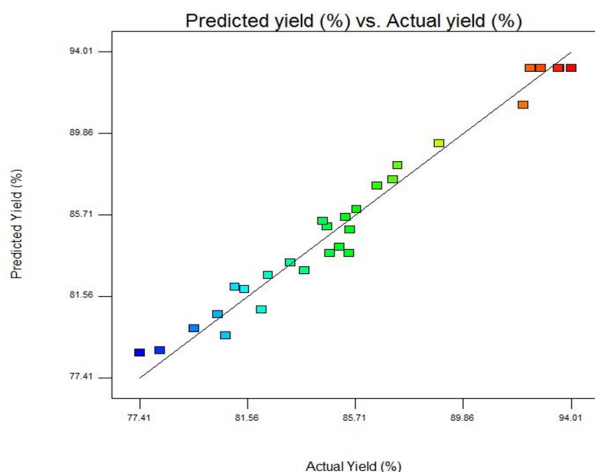

Figure 1. Actual versus predicted value for biodiesel yield.
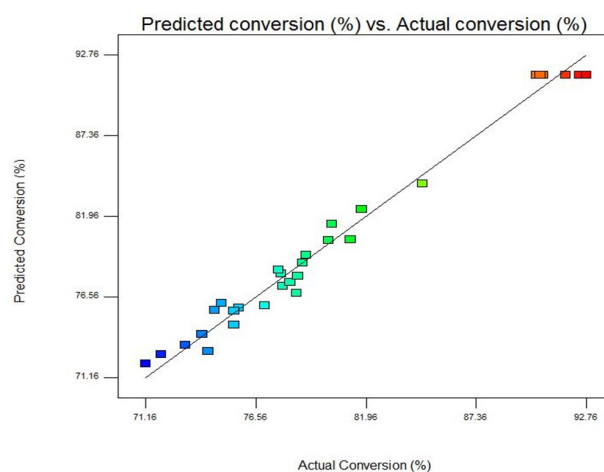

Figure 2. Actual versus predicted value for biodiesel conversion.

mass transfer limitations problem, similar to the situation reported by Namdeo [14]. This mass transfer limitation problem can be avoided by applying stirring on the system [15]. Optimum stirring for sulfonation enhances the attachment of $-SO_3H$. Noureddini and Zhu proposed an initial mass transfer controlled region followed by a kinetically controlled region for base catalytic transesterification of sunflower oil [16]. Hou *et al.* showed that the reaction is very slow initially due to mass transfer limitations between methanol and oil phase [17].

The distinction between the experimental data as well as the predicted data for both Y and C are illustrated in Figures 1 and 2, respectively. Based on Figure 1, a slight deviation was shown from $Y_{act} = Y_{pred}$, where Y_{act} is referring to experimental data meanwhile Y_{pred} is the data predicted for Y. The slight deviation proves the relevancy of the generated model which appropriately aligned with the model generated. The predicted values lie near the plotted line which contributing to higher value of R^2. This is almost the same with Figure 2

where $C_{act} = C_{pred}$ where C_{act} referring to the conversion from experimental value meanwhile C_{pred} is the predicted value from the modelling. Figure 2 shows that the regression model develop is appropriate.

Residuals on the other hand is the difference between Y_{act} and Y_{pred} as well as C_{act} and C_{pred}. Residuals are estimation of experimental error obtained by subtracting the observed responses from the predicted responses. Normal probability plot of the residuals is a method to learn whether it is reasonable to assume the error terms are normally distributed. Normal distributions are achieved when the residuals values fall onto the linear line. Based on Figures 3 and 4, the normal distribution were achieved and satisfied both yield and conversion where the line adjacently located to the straight line.

The effect of each variables on the Y and C can be evaluated from the Pareto chart. Pareto charts visually represents the absolute values of the effects of main factors and the effects of interaction of factors. The chart includes a ver-
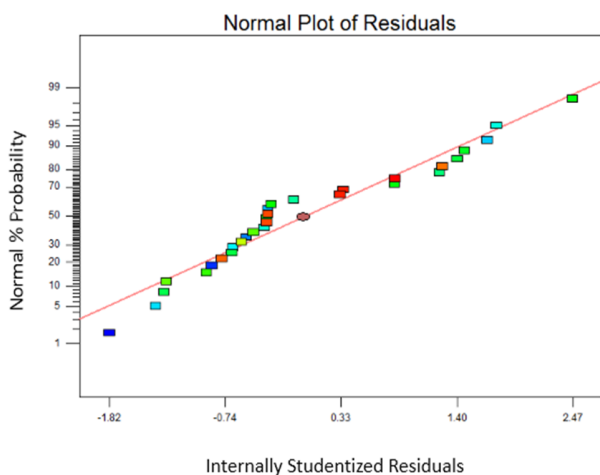

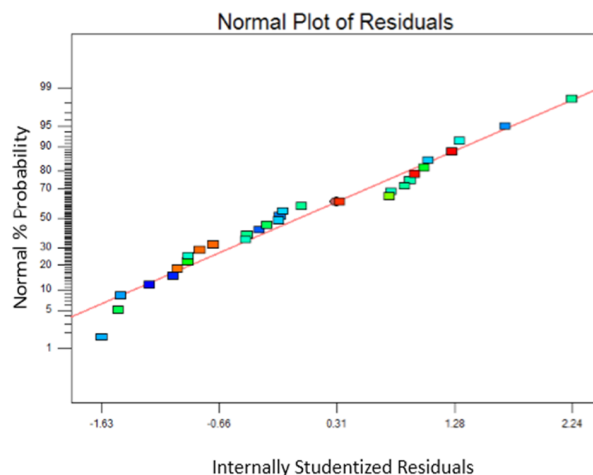**Figure 3.** Normal plot of residuals for biodiesel yield.

Figure 4. Normal plot of residuals for biodiesel conversion.
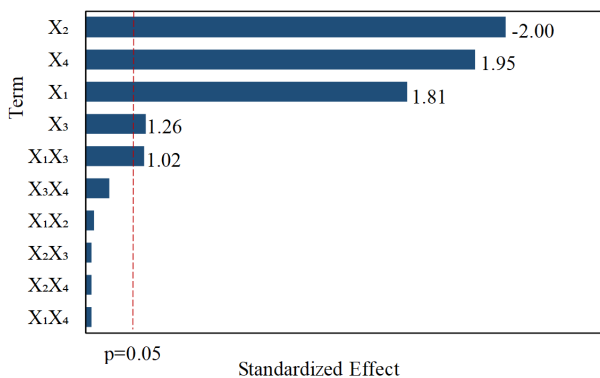

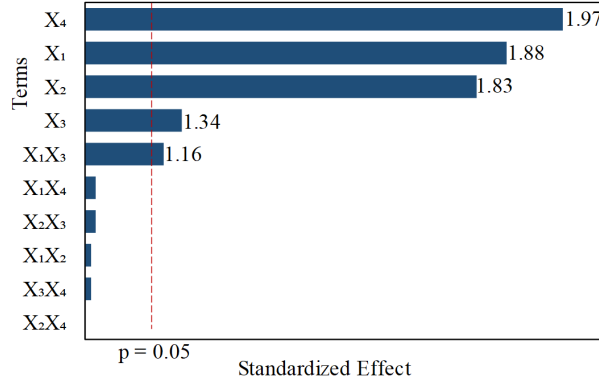**Figure 5.** Pareto chart for biodiesel yield.


Figure 6. Pareto chart for biodiesel conversion.

tical reference line at the critical *t*-value for an alpha of 0.05 (magnitude for a 95% confidence level) to indicate that the factors which extend past this line are potentially important. From Figure 5 and Figure 6, all effects are statistically significant.

The significance of the interaction between effects could also be compared from the Pareto charts. Significance positive effects was identified in the interaction between the time and power level. These plots clearly indicated that the significance of the variables and their interaction between effects towards *Y* and *C* decreased in this order, $X_2 > X_4 > X_1 > X_1X_3 > X_3$ and $X_4 > X_1 > X_2 > X_3 > X_1X_3$, respectively. Kefas and colleagues also did an optimization for sulfonation of glucose catalyst [18]. Four independent variables used including heating time (*A*), concentration of $(NH_4)_2SO_4$ (*B*), Volume of H_2SO_4 (*C*) and Temperature (*D*). However, based on the optimization result, parameter *B* and *A* were found to be the most significant with lowest *p*-value (< 0.05). The sulfonation of ICG using $(NH_4)_2SO_4$ heated conventionally within 1 to 9 hour was proven to be effective for attachment of $-SO_3H$ groups to the polycyclic aromatic structure of the ICG, thus producing a high number of surface area of 4.47 m^2/g with acid density of 5.92 mmol/g, lower from the catalyst prepared using microwave-heating method. The highest surface area from the best performing catalyst, from our previous report [10], was recorded at 16.94 m^2/g with acid density of 25.65 mmol/g. In fact, the prepared catalyst using microwave-heating system reducing lots of time consumed during sulfonation process and thus reducing the cost for electricity.

3.2 Response Surface Contour Plot

The response between two factors can be determined via contour plots, 3D surface or cube surface in design expert software by observing the effects as well as interaction of the response from the two variables. Figures 7 to 18 show the contour plots for every possible interaction between two independent parameters while the other two variables is kept at the center of their respective range.

Figures 7 and 8 portrays contour plots for interaction between volume of H_2SO_4 and time (min) where both power level (W) and stirring rate (rpm) were constant at 400 W and 600 rpm, respectively. The increment of *Y* and *C* were observed as the H_2SO_4 volume increased right until it slightly reduce after 163 ml and 160 mL of H_2SO_4 used. The presence of large quantity of H_2SO_4 increase the number of acid active sites available for reaction to occur, but excessive H_2SO_4 negatively impact *Y* value possibly due to great structural destruction that lead to less surface for $-SO_3H$ group attachment. Similar case is observed for heating time. *Y* increased with the increase of heating time. The 7 to 8 minutes is found to be the optimum value for heating time of catalyst in microwave to obtained maximum *Y*. Prolonged the catalyst heating time more than 8 minute negatively impact the catalytic activity of catalyst as the surface of catalyst may saturated with the $-SO_3H$ group that will hinder methanol react with the active sites [19]. The contour plot is portrayed in oval or elliptical shape which is proven by Erbay and colleagues as a perfect interaction between the independent variables [20].
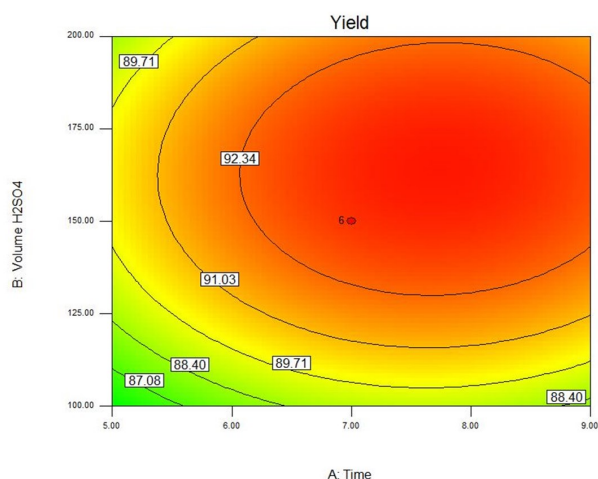
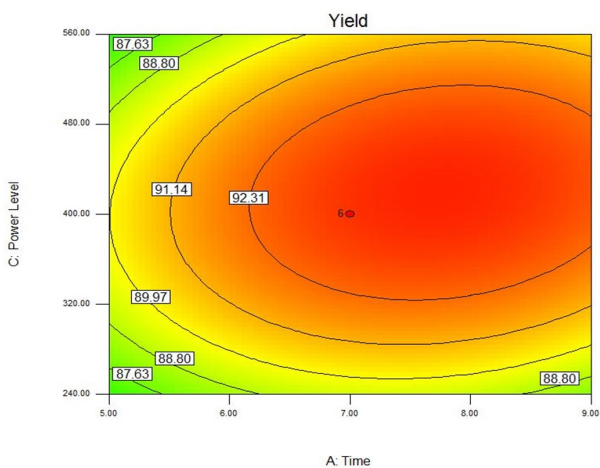**Figure 7.** Yield contour plot time (min) against volume H_2SO_4 (mL) for catalyst heated at 400 W and 600 rpm stirring rate.
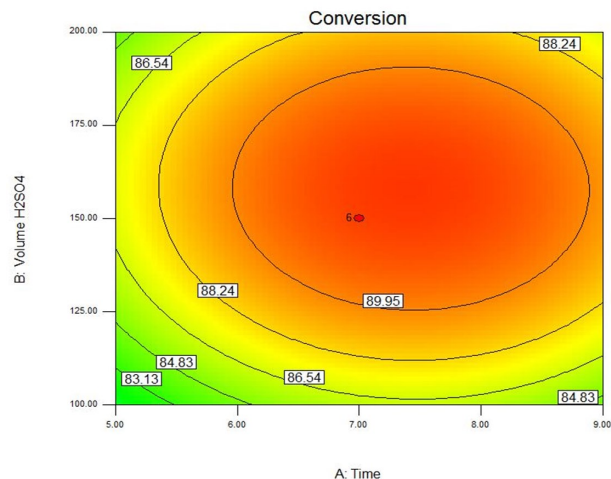
Figure 8. Conversion contour plot time (min) against volume H_2SO_4 for catalyst heated at 400 W and stirred at 600 rpm.

Figures 9 and 10 depicts the contour plots of time (min) against power level (W) of microwave to obtain an optimum Y and C, respectively. The 150 mL volume of H_2SO_4 and 600 rpm stirring rate were fixed at this rate. Percentage Y and C were increased as heating time increased with 7.65 min and 7.49 min of optimum heating time (min) recorded based on the graph, respectively. As heating time increased from 5 min to 7 min, the yield and conversion percentage of the biodiesel increased indicating a pretty fast sulfonation process. The peak value appears around 7.65 min and 7 min for both Y and C, over which further prolonging the sulfonation makes no obvious sense. Theoretically, a sulfonation process requires certain duration to be connected with sulfonic acid groups from concentrated sulfuric acid to the carbon frames. Once the process is done, further prolonging the duration makes no sense. The same occurs with the power level (W) as Y and C amplified with the increment of the power level and started to reduce when the power level reached 400 W. A high power level hinder the $-SO_3H$ group incorporated into the carbon network of catalyst [21]. The optimum range of the power level is located between 320 W to 480 W.

Figures 11 and 12 show the effect and interaction of time and stirring rate for both Y and C. From the contour plot of both graph, the value of Y and C continue to increase with the increment in time of catalyst heating. The interaction between Y or C and the stirring rate also
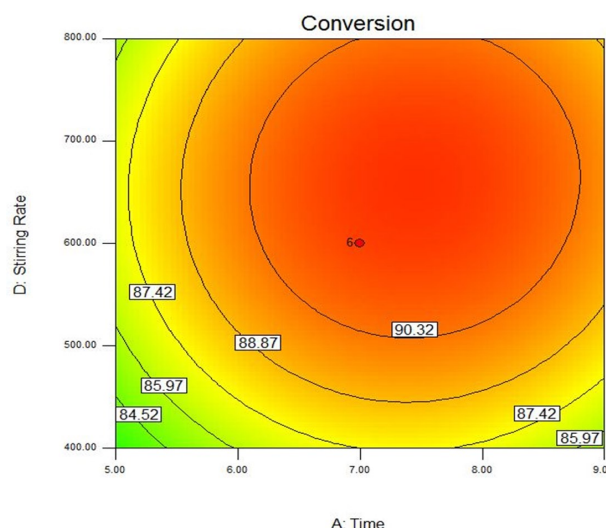

Figure 9. Yield contour plot time (min) against power level (W) for catalyst prepared with 150 mL H_2SO_4 and 600 rpm stirring rate.
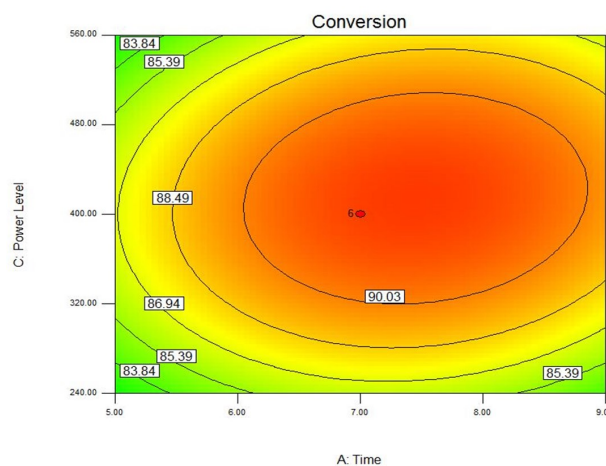
Figure 10. Conversion contour plot time (min) against power level (W) for catalyst prepared using 150 mL and stirred at 600 rpm.
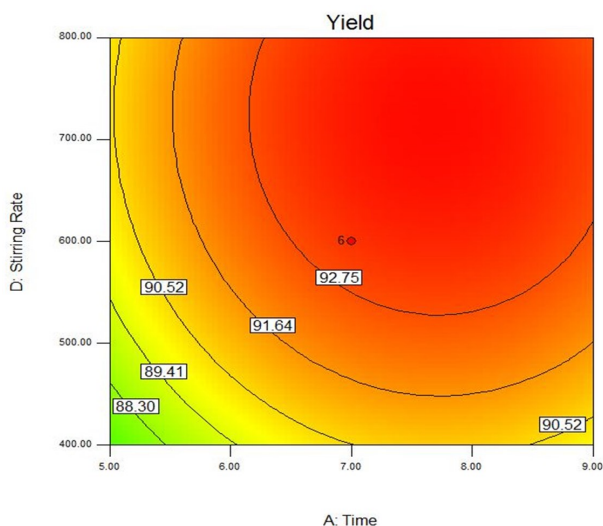
Figure 11. Yield contour plot time (min) against stirring rate (rpm) for catalyst heated at 400 W and using 150 mL H_2SO_4.

Figure 12. Conversion contour plot time (min) against stirring rate (rpm) for catalyst heated at 400 W and using 150 mL H_2SO_4.

demonstrate the same pattern in which any increasing in stirring rate value results in inclination of Y or C. It can be observed that to get maximum value of responses, the optimum value of heating time for catalyst as well as stirring rate is 718.92 rpm and 7.65 min for Y and 659.46 rpm with 7.49 min for C. This is practically due to the mass transfer limitation problem as discussed previously. Optimum stirring rate for sulfonation induced the probability of attachment of $-SO_3H$.

As for effect and interactions between volume of H_2SO_4 and power level, a plotted contour plot was presented in Figure 13 and Figure 14. The graph shows an increment in value of Y and C as the volume of H_2SO_4 used to sulfonate the catalyst increase. However, the Y value started to decrease after the usage of H_2SO_4 volume reached 160 mL. The same pattern of response is also observed through the interactions between power levels with Y and C. With the increasing in value of power level parameter, Y and C also increase, before started to decrease at power level value of 420 W. The highest temperature from the highest power level might lead to an excessive breakdown of the macromolecules and removal of organic portions [22].

While keeping the time for catalyst heating 7 minutes and power level 400 W, the effect and interactions between volume of H_2SO_4 used and stirring rate with Y is demonstrated in Figure 15 and Figure 16. From the graph, it can be seen that the value of Y increase and decrease as the volume of H_2SO_4 used to sulfonate the glucose is increased, with optimum value of Y is obtained at 160 mL. As for the effects and interactions of stirring rate to Y val-
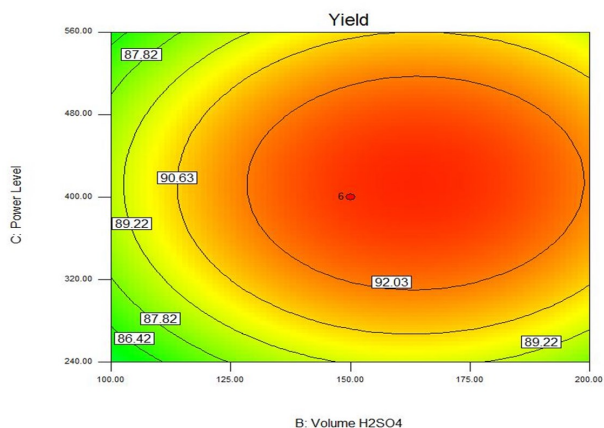

Figure 13. Yield contour plot volume H_2SO_4 (mL) against power level (W) for catalyst heated at 7 min and stirred at 600 rpm.
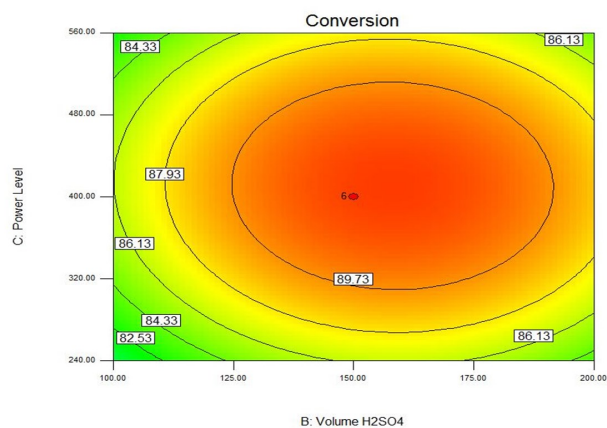

Figure 14. Conversion contour plot volume H_2SO_4 (mL) against power level (W) for catalyst heated for 7 min and stirred at 600 rpm.
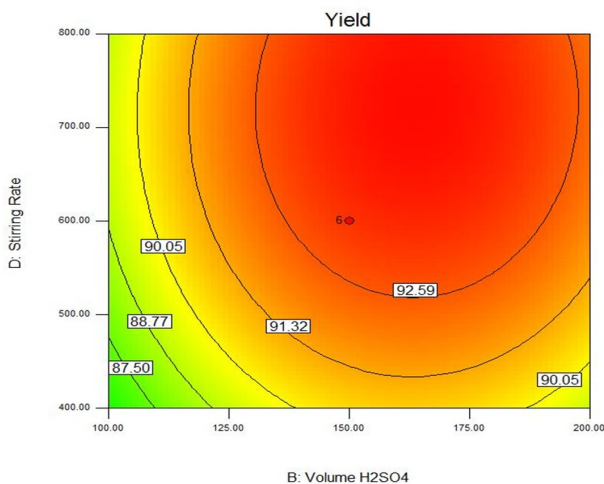

Figure 15. Yield contour plot volume H_2SO_4 (mL) against stirring rate (rpm) for catalyst heated at 400 W for 7 min.
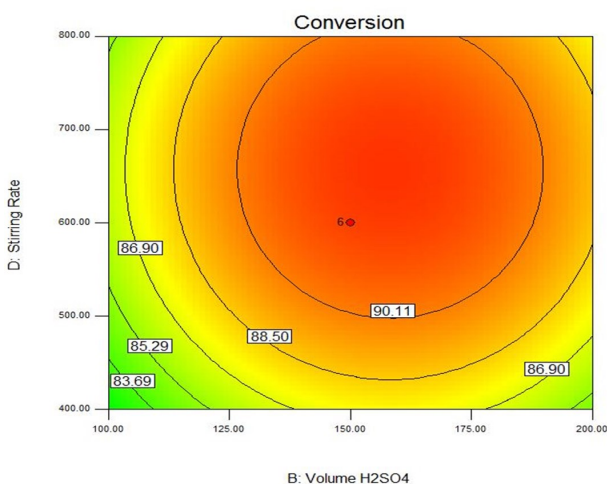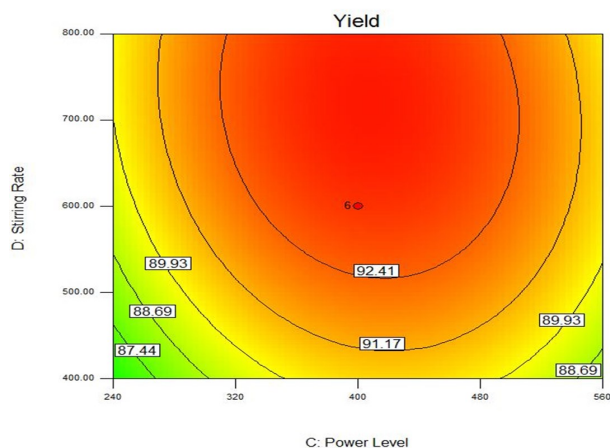

Figure 16. Conversion contour plot volume H_2SO_4 (mL) against stirring rate (rpm) for catalyst heated at 400 W for 7 min.

ue, the increment of stirring rate causes Y value to increase up until 700 rpm before the pattern started to decrease. Efficient stirring rate with sufficient volume of H_2SO_4 effectively reduced the initial mass transfer limitation caused by the polar and non-polar of H_2SO_4 and D(+)-glucose structure. Thus, optimum stirring rate enhanced the attachment of $-SO_3H$ group to the D(+)-glucose surface yet increase the Y and C value. High stirring rate was not applicable due to the spillage of the solution thus reducing the volume of the H_2SO_4.

The effect and interaction of power level and stirring rate towards Y were also studied through the contour plot, as illustrated in Figure 17 and Figure 18. It can be seen that Y and C shows an increasing pattern as the power level increase up to 400 W before it started declining. The microwave power level should not

be too high, as it might cause a sharp rise in reaction temperature, resulting in more accumulated discontinuities and shortened molecular reorientation and vibration times. In contrast, if microwave output was too low, most of the microwave power would be used to warm up the reaction mixture, and the temperature would be lower than required in most cases, resulting in a lower yield. The appropriate microwave power density and its dissipation control were very important to maximize ester yield and minimize reaction time and microwave energy consumption [23].

Optimum value is the ideal value of the variables obtained when the highest Y and C is achieved. The optimum value of Y and C is tabulated in Table 5. The highest yield and conversion can be achieved is 94.01% and 91.89% respectively at optimum operating condition of

Figure 17. Yield Contour Plot power level (W) against stirring rate (rpm) for catalyst heated for 7 min using 150 ml H_2SO_4.
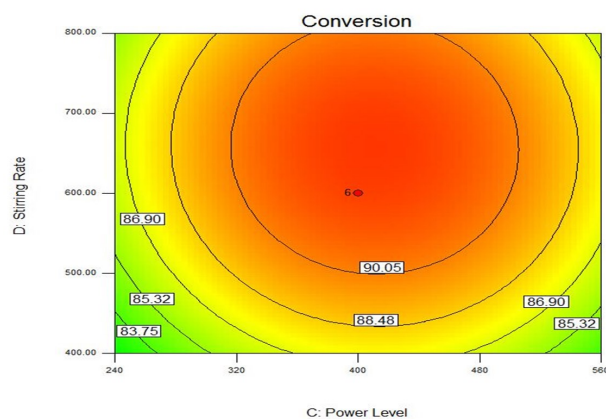
Figure 18. Conversion Contour Plot power level (W) against stirring rate (rpm) for catalyst heated for 7 min and using 150 ml of volume H_2SO_4.

Table 5. Optimum operating condition to produce maximum Y.

Parameters	Time (min)	Volume of H_2SO_4 used (mL)	Power level (W)	Stirring rate (rpm)	Max Y (%)	Max C (%)
	7.53	159.51	413.64	670.53	94.01	91.89

Table 6. Validation test for yield using optimum value from optimization.

No	Operation Condition of Optimum Value				Yield (%)	Conv (%)
	Time (min)	Volume of H_2SO_4 (ml)	Power Level (W)	Stirring rate (rpm)		
1					90.31	87.46
2	7.5	160	400	700	92.06	89.09
3					92.89	88.74
	Average				91.75	88.43

7.5 min for time of heating catalyst, 159.5 mL of H_2SO_4, 413.6 W of power level, and stirring rate of 671 rpm.

The optimum result was then validated by conducting confirmatory experiment and the results are presented in Table 6. There are some limitation for validation test for optimum value. 3 replicate experiments had been done to validate the optimum value however, the experimental work was done using power level of 400 W and stirring rate at 700 rpm, since the automated function of the equipment cannot be set to the respective value. The average of the validation test was a bit off from the predicted optimum value since the variables such as microwave power level and stirring rate is according to analogue system and cannot be modified with the respective optimum value. The validation test obtained 91.75% and 88.43% for Y and $C,$ respectively.

4. Conclusions

Response surface methodology was used optimized and study the effect of the sulfonation process of synthesizing SO_3H/ICG acid catalyst via microwave heating method. Quadratic model was proposed for prediction of biodiesel yield (Y) from palm fatty acid distillate (PFAD) and its conversion (C). The application of DOE successfully optimized the operating conditions for the two-step SO_3H/ICG catalyst synthesis to be used for the esterification process. The optimized conditions of the best performing SO_3H/ICG with maximum Y and C were at 7.53 minutes of reaction time, 159.5 mL of H_2SO_4 used, 671 rpm of stirring rate as well as 413.6 watt of power level. At these optimum conditions the predicted yield percentage and conversion percentage were 94.01% and 91.89%. The utilization of sulfonated glucose solid acid catalyst via microwave-assisted in biodiesel production has great potential towards sustainable and green method of synthesizing catalyst for biodiesel. The preparation of the catalyst is much convenient in time and energy consumption.

Acknowledgments

References

[1] Anwar, M., Rasul, M.G., Ashwath, N. (2018). Production optimization and quality assessment of papaya (Carica papaya) biodiesel with response surface methodology. *Energy Conversion and Management*, 156, 103–112, doi: 10.1016/j.enconman.2017.11.004

[2] Zong, M.-H., Duan, Z.-Q., Lou, W.-Y., Smith, T.J., Wu, H. (2007). Preparation of a sugar catalyst and its use for highly efficient production of biodiesel. *Green Chemistry*, 9(5), 434–437, doi: 10.1039/B615447F

[3] Lokman, I.M., Rashid, U., Taufiq-Yap, Y.H., Yunus, R. (2015). Methyl ester production from palm fatty acid distillate using sulfonated glucose-derived acid catalyst. *Renewable Energy*, 81, 347–354, doi: 10.1016/j.renene.2015.03.045

[4] Shuit, S.H., Tan, S.H. (2014). Feasibility study of various sulphonation methods for transforming carbon nanotubes into catalysts for the esterification of palm fatty acid distillate. *Energy Conversion and Management*, 88, 1283–1289, doi: 10.1016/j.enconman.2014.01.035

[5] de Almeida, V.F., Garcia-Moreno, P.J., Guadix, A., Guadix, E.M. (2015). Biodiesel production from mixtures of waste fish oil, palm oil and waste frying oil: Optimization of fuel properties. *Fuel Processing Technology*, 133, 152–160, doi: 10.1016/j.fuproc.2015.01.041

[6] Awad, S., Paraschiv, M., Varuvel, E.G., Tazerout, M. (2013). Optimization of biodiesel production from animal fat residue in wastewater using response surface methodology. *Bioresource Technology*, 129, 315–320, doi: 10.1016/j.biortech.2012.11.086

[7] Lokman, I.M., Rashid, U., Taufiq-Yap, Y.H. (2015). Production of biodiesel from palm fatty acid distillate using sulfonated-glucose solid acid catalyst: Characterization and optimization. *Chinese Journal of Chemical Engineering*, 23(11), 1857–1864, doi: 10.1016/j.cjche.2015.07.028

[8] Mohamad, N., Huyop, F., Aboul-Enein, H.Y., Mahat, N.A., Wahab, R.A. (2015). Response surface methodological approach for optimizing production of geranyl propionate catalysed by carbon nanotubes nanobioconjugates. *Biotechnology & Biotechnological Equipment*, 29(4), 732–739, doi: 10.1080/13102818.2015.1034177

[9] Jiménez Toro, M.J., Dou, X., Ajewole, I., Wang, J., Chong, K., Ai, N., Zeng, G., Chen, T. (2019) Preparation and Optimization of Macroalgae-Derived Solid Acid Catalysts. *Waste and Biomass Valorization*, 10(4), 805–816, doi: 10.1007/s12649-017-0101-0

[10] Saimon, N.N., Eu, H.K., Ngadi, N., Jusoh, M., Johari, A., Zakaria, Z.Y. (2018). Production of Biodiesel from Palm Fatty Acid Distillate by Microwave-Assisted Sulfonated Glucose Acid Catalyst. *Sains Malaysiana*, 47(1), 109–115, doi: 10.17576/jsm-2018-4701-13

[11] Reale, S. (1993). Design and analysis of experiments: Third Edition. By Douglas C. Montgomery. John Wiley, *Chichester International Journal of Pressure Vessels and Piping*, 53(2), 359–360.

[12] Cornell, J.A. (1990). *How to Apply Response Surface Methodology*. Winconsin: ASQS.: American Society for Quality Control Statistics Division.

[13] Lee, H.V., Yunus, R., Juan, J.C., Taufiq-Yap, Y.H. (2011). Process optimization design for jatropha-based biodiesel production using response surface methodology. *Fuel Processing Technology*, 92(12), 2420–2428, doi: 10.1016/j.fuproc.2011.08.018

[14] Namdeo, A., Jhaveri, J., Mahajani, S.M., Suresh, A.K. (2018). Effect of mass transfer limitation on catalytic activity and selectivity for oxidation of glycerol. *International Conference on Chemical Reaction Engineering*.

[15] Roy, P.K., Datta, S., Nandi, S., Al-Basir, F. (2014). Effect of mass transfer kinetics for maximum production of biodiesel from Jatropha Curcas oil: A mathematical approach. *Fuel*, 134, 39–44, doi: 10.1016/j.fuel.2014.05.021

[16] Noureddini, H., Zhu, D. (1997). Kinetics of transesterification of soybean oil. *Journal of the American Oil Chemists' Society*, 74(11), 1457–1463, doi: 10.1007/s11746-997-0254-2

[17] Hou, X., Qi, Y., Qiao, X., Wang, G., Qin, Z., Wang, J. (2007). Lewis acid-catalyzed transesterification and esterification of high free fatty acid oil in subcritical methanol. *Korean Journal of Chemical Engineering*, 24, 311–313, doi: 10.1007/s11814-007-5052-x

[18] Kefas, H.M., Yunus, R., Rashid, U., Taufiq-Yap, Y.H. (2018). Modified sulfonation method for converting carbonized glucose into solid acid catalyst for the esterification of palm fatty acid distillate. *Fuel*, 229, 68-78, doi: 10.1016/j.fuel.2018.05.014

[19] Endut, A., Abdullaah, S.H.Y.S., Hanapi, N.H.M., Hamid, S.H.A., Lananan, F., Kamarudin, M.K.A., Umar, R., Juahir, H., Khatoon, H. (2017). Optimization of biodiesel production by solid acid catalyst derived from coconut shell via response surface methodology. *International Biodeterioration & Biodegradation*, 124, 250−257, doi: 10.1016/j.ibiod.2017.06.008

[20] Erbay, Z., Icier, F. (2009). Optimization of hot air drying of olive leaves using response surface methodology. *Journal of Food Engineering*, 91(4), 533−541, doi: 10.1016/j.jfoodeng.2008.10.004

[21] Ning, Y., Niu, S. (2017). Preparation and catalytic performance in esterification of a bamboo-based heterogeneous acid catalyst with microwave assistance. *Energy Conversion and Management*, 153, 446–454, doi: 10.1016/j.enconman.2017.10.025

[22] Wei, Z., Xiong, D., Duan, P., Ding, S., Li, Y., Li, L., Niu, P., Chen, X. (2020). Preparation of Carbon-Based Solid Acid Catalysts Using Rice Straw Biomass and Their Application in Hydration of α-Pinene. *Catalysts*, 10(2), 213, doi: 10.3390/catal10020213

[23] Chen, H.-Y., Cui, Z.-W. (2016). A Microwave-Sensitive Solid Acid Catalyst Prepared from Sweet Potato via a Simple Method. *Catalysts*, 6(12), 211, doi: 10.3390/catal6120211